

Linking Theory to Practice: Predicting Ballistic Performance from Mechanical Properties of Aged Body Armor

Amanda L. Forster¹, Dennis D. Leber², Amy Engelbrecht-Wiggans^{1,3}, Virginie Landais¹, Allen Chang¹, Emilien Guigues¹, Guillaume Messin¹, and Michael A. Riley¹

¹Material Measurement Laboratory,
National Institute of Standards and Technology,
Gaithersburg, MD 20899, USA

²Information Technology Laboratory,
National Institute of Standards and Technology,
Gaithersburg, MD 20899, USA

³Theiss Research,
La Jolla, CA 92037, USA

Amanda.forster@nist.gov
Dennis.leber@nist.gov
Amy.engelbrecht-wiggans@nist.gov
Virglandais@gmail.com
Allenchang@mail.pse.umass.edu
Emilien.guigues@outlook.com
Guillaume.messin@gmail.com
Michael.Riley@nist.gov

It has long been a goal of the body armor testing community to establish an individualized, scientific-based protocol for predicting the ballistic performance end of life for fielded body armor. A major obstacle in achieving this goal is the test methods used to ascertain ballistic performance, which are destructive in nature and require large sample sizes. In this work, using both the Cunniff and Phoenix-Porwal models, we derived two separate but similar theoretical relationships between the observed degradation in mechanical properties of aged body armor and its decreased ballistic performance. We present two studies used to validate the derived functions. The first correlates the degradation in mechanical properties of fielded body armor to the degradation produced by a laboratory accelerated-aging protocol. The second examines the ballistic resistance and the extracted-yarn mechanical properties of new and laboratory-aged body armor made from poly(*p*-phenylene-2,6-benzobisoxazole), or PBO, and poly(*p*-phenylene terephthalamide), or PPTA. We present correlations found between the tensile strengths of yarns extracted from armor and the ballistic limit (V_{50}) when significant degradation of the mechanical properties of the extracted yarns was observed. These studies provided the basis for a validation data set in which we compared the experimentally measured V_{50} ballistic limit results to the theoretically predicted V_{50} results. The theoretical estimates were generally shown to provide a conservative prediction of the ballistic performance of the armor. This approach is promising for the development of a tool for fielded armor performance surveillance relying upon mechanical testing of armor coupon samples.

Key words: artificial aging; ballistic resistance; body armor; field aging.

Accepted: August 3, 2020

Published: August 24, 2020

<https://doi.org/10.6028/jres.125.026>

1. Introduction

In the wake of a 2003 field failure of a piece of body armor composed of poly(*p*-phenylene-2,6-benzobisoxazole) [1–3], or PBO, questions have been raised regarding the expected service life of ballistic-resistant body armor. A study conducted prior to 1990 on body armor made from poly(*p*-phenylene terephthalamide), or PPTA, indicated that armor that had been in use for approximately 10 years could still defeat the threats it was designed to stop [4]. The conclusion in this 1986-published study is no longer applicable because the armor used in that study is not representative of the materials and construction techniques that are used in modern body armor. For the last decade, the body armor community has conducted major research efforts to understand the effects of field and laboratory aging on the performance of body armor [5–7]. These efforts culminated in a revised standard [8] for ballistic-resistant body armor that included an environmental conditioning protocol to test the capability of a given armor design to withstand conditions of heat, moisture, and mechanical wear, which may translate to enhanced confidence in the long-term performance of the armor.

To assess the long-term field performance of armor, an ideal study would consist of issuing a single body armor design to thousands of end users who work in an array of different types of positions (e.g., patrol officers vs. detectives) in a diversity of climates (e.g., southern United States vs. northern Canada). Armor would then be removed from service for analysis at specified intervals. Unfortunately, this ideal study has proven difficult to execute in practice because no single design of body armor has ever been issued to a large number of end users. In reality, law enforcement officers in the United States and across the world utilize a variety of different armor designs. Furthermore, the actual use condition for an individual piece of armor is incredibly challenging to precisely assess: Officers can be reassigned or promoted over the course of a few years of service, thus changing the use of their armor; some officers do not wear their armor regularly; and some officers may not follow common standards of care for their armor (e.g., some may hang it when it is not being worn, while others may leave it in the bottom of their locker or the trunk of their car until it is needed again).

A study of field-aged armor was conducted in Canada [9, 10]; however, interpretations of the data were complicated because of the wide variety of armor designs sampled. The study was further complicated by the difficulty inherent in assessing the performance of the armor at the end of its life cycle without a consistent and accurate benchmark for the performance of that armor when it was new. The benchmark used was of questionable accuracy due to the limited number and placement of shots required at the time to assess the armor performance when it was new, as specified by previous versions of the National Institute of Justice (NIJ) body armor standard to which the armor was originally certified, but since revised, as is discussed later herein. These issues, and the variability that resulted in benchmark values, led the authors of the Canadian study to conclude that correlations could not be established between armor age and ballistic performance.

Most armor sold in the United States for use by law enforcement officers has a 5 year warranty period. Typically, one would expect body armor to be designed with a “safety margin” to account for the potential of a reduction in armor performance over time due to use and wear [1–3]. Because of the aforementioned variations in armor design, use, and care, such a warranty period and expected safety margin cannot be uniformly assumed to be analogous with “safe for use” across the population of fielded armor. This individuality of fielded body armor presents substantial challenges for organizations in defining effective armor surveillance and replacement policies. While performing a large-scale study to examine fielded armor performance remains challenging, we attempted herein to combine available data from fielded and laboratory-aged armor to better understand armor long-term performance, where the focus was on correlating the measured tensile strength of component yarns to the armor’s measured ballistic limit (V_{50}), whether new or aged.

The V_{50} is defined by ASTM Standard E3110-18 as “the velocity at which 50 % of the impacts by a specified test threat are expected to completely penetrate nominally identical test items when tested

according to a specified test method” [11]. The V_{50} provides a convenient mechanism to track relative changes in ballistic performance that might not be revealed by a perforation test, which only investigates the ability of an armor to stop threats of a specified velocity.

Using a logistic regression model to describe the probability of perforation, Fig. 1 illustrates the ballistic performance differences between new and aged armor. The details of the application of the logistic regression analysis to V_{50} data are reported elsewhere [8, 12]. Figure 1 shows the probability-of-perforation curves for a new PBO armor and for a PBO armor of the same model after being artificially aged using the conditioning protocol described in NIJ Standard 0101.06 [8].

The NIJ Standard 0101.04 [13] threats were used in this investigation because they matched the conditions of a known field failure for PBO body armor. This standard defines a “fair hit” velocity, for a 9 mm, 8.04 g full-metal-jacket projectile for the “fair hit” range, as a shot with a velocity of $341 \text{ m/s} \pm 9.1 \text{ m/s}$. This fair hit range is indicated in Fig. 1. We note that the estimated probability of perforation at the upper bound of the fair hit velocity interval (350.1 m/s) for the new armor is about 0.04 %, with an upper 95 % confidence bound of 3.7 %. The estimated V_{50} provided by the logistic model for the new armor is 458 m/s, which exceeds the upper bound of the fair hit velocity interval, 350.1 m/s, by about 31 %. In contrast, for the aged armor, the estimated probability of perforation at the upper bound of the fair hit velocity interval is approximately 0.6 %, with an upper 95 % confidence bound of 8.9 %. Furthermore, the estimated V_{50} for the aged armor, which is 416 m/s, exceeds the upper bound, 350.1 m/s, of the fair hit velocity interval by about 19 %. Both the downward shift in V_{50} and the upward shift in the probability of perforation at the upper bound of the fair hit velocity interval for aged armor, as compared to new armor, indicate that the ballistic performance of the armor has declined with aging. This example signifies the importance of investigating the effect of aging on armor systems.

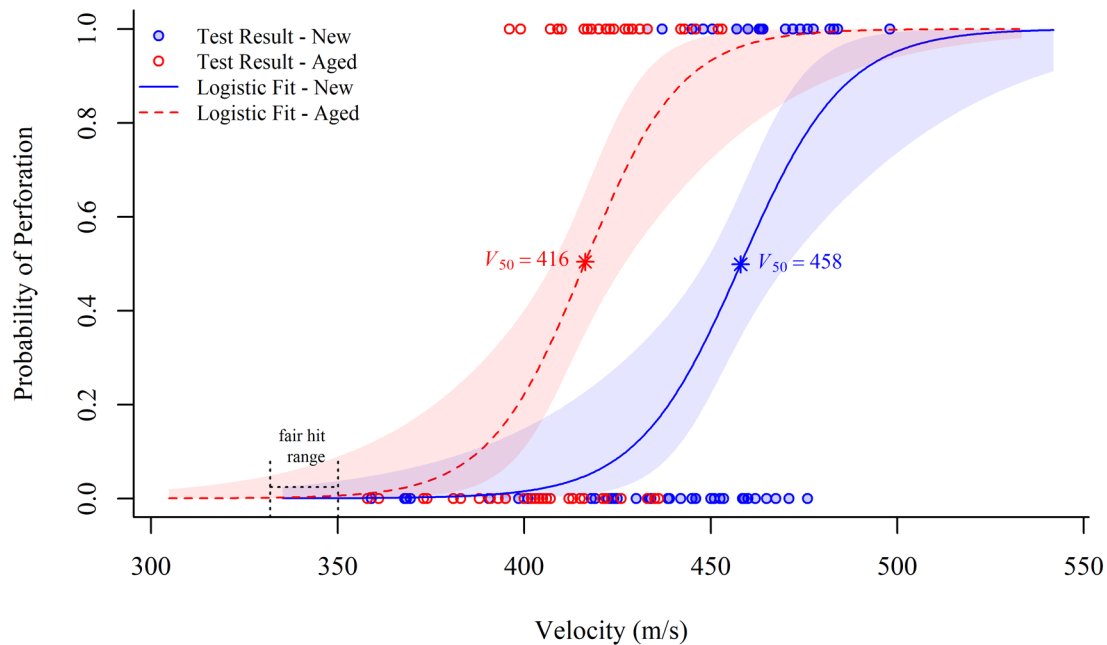


Fig. 1. Logistic regression models for the probability of perforation for new and aged PBO body armor. The circles represent the threat velocity and perforation result (1 = perforation, 0 = no perforation) of the V_{50} test. The shaded regions are the 95 % confidence intervals of the logistic regression fit.

Beyond the logistic regression modeling of empirical V_{50} test results, there are theoretical methods for considering the influence of material properties on ballistic performance [14–19]. These methods focus on the concepts of strain-wave speed and specific toughness. The strain-wave speed represents the speed of

energy dissipation away from a point of ballistic impact, and the specific toughness represents the approximate amount of elastic energy a fiber can withstand or absorb before failure, as normalized by mass. In an effort to combine these concepts into one term, which can be expressed as a ballistic property (a theoretical V_{50}), Cunniff determined a relationship between dimensionless parameters based on extensive experimental data [15]. Phoenix and Porwal also related the concepts of strain wave, specific toughness, and V_{50} and developed a theoretical membrane model for an in-plane isotropic material [16–18].

In the following sections, we leveraged the works of Cunniff and Phoenix-Porwal to derive two separate, but similar theoretical models that relate a decrease in the material properties of yarns used in armor to a decrease in the armor's V_{50} . We then describe a study that links the mechanical properties of artificially aged armor with those of field-aged armor. This is followed by further study of the artificially aged armor wherein a positive correlation between tensile strength of yarns extracted from the armor and the V_{50} ballistic limit was observed. This work formed the basis for the data set used in the validation of our derived models. We conclude with suggestions on how these results might facilitate an individualized armor surveillance program.

2. Derivation of Theoretical Degradation Relationships

The results of different theoretical studies agree in that the concepts of specific toughness and strain-wave speed are critical in predicting ballistic performance [14–16, 20]. The strain-wave speed is the speed of energy dissipation away from a point of ballistic impact and is calculated as the square root of the ratio of a fiber's Young's modulus, E , to the fiber density, ρ : $\sqrt{E/\rho}$. Specific toughness is the approximate amount of stored elastic energy a fiber can withstand before failure, as normalized by mass density, and it is calculated as the ratio of the product of fiber ultimate axial tensile strength, σ , and fiber ultimate tensile strain, ε , over twice fiber density: $\sigma\varepsilon/(2\rho)$. The mechanical properties of a fiber can be readily determined from tensile testing, so the relationships between fiber properties and ballistic performance can, in theory, allow for prediction of a material's ballistic performance based on simple tests. Full details of this analysis are given in another publication [21], and a brief summary is also included below.

2.1 Cunniff's Tensile-Strength-to- V_{50} Relation

Cunniff's paper [15] examined a large base of experimental data, aiming to determine relationships between material properties and V_{50} that hold for different materials. The variables of interest that he identified were the fiber toughness, fiber strain-wave velocity, V_{50} , and a ratio, Γ_0 , of projectile and system areal density,

$$\Gamma_0 = \frac{A_d A_p}{m_p}, \quad (1)$$

where A_d is the armor system areal density, A_p is the projectile presented area to the target, and m_p is the projectile mass. He then used dimensional analysis of the experimental V_{50} data obtained over a wide range of parameter values (including projectile and target dimensions and masses and fiber mechanical properties and densities) to determine a function, Φ , between two dimensionless parameters that resolved and fit the experimental data for all but one of the material systems of interest, namely:

$$\Phi\left(\Gamma_0, \frac{V_{50}}{\Omega^{1/3}}\right) = 0, \quad (2)$$

where Ω is the product of the material's specific toughness with the strain-wave velocity:

$$\Omega = \frac{\sigma \varepsilon}{2\rho} \sqrt{\frac{E}{\rho}}. \tag{3}$$

Aging the material can cause changes in its mechanical properties, such as ultimate tensile strength, ultimate tensile strain, and Young's modulus, but the material density is assumed to stay constant. (This assumption was verified in Ref. [22], where density was found to be independent of water sorption/desorption.) The ratio of the V_{50} of aged material to that of unaged material, for a constant projectile type, can then be calculated as a function of these material parameters as follows: For fixed projectile type, the areal density ratio, Γ_0 , is constant, so the second dimensionless term in Eq. (2) must also remain constant because Eq. (2) is bijective. Thus, V_{50} is proportional to the cubed root of Ω :

$$V_{50C} \propto \Omega^{1/3}, \tag{4}$$

where the "C" subscript refers to the Cunniff model. Writing this for both aged and unaged material and taking the ratio yields the percent retention of V_{50} for the Cunniff model, rV_{50C} ,

$$\begin{aligned} rV_{50C} &= \frac{V_{50C \text{ aged}}}{V_{50C \text{ new}}} \times 100 = \left(\frac{\Omega_{\text{aged}}}{\Omega_{\text{new}}} \right)^{\frac{1}{3}} \times 100 = \left(\frac{\sigma_{\text{aged}} \varepsilon_{\text{aged}}}{2\rho} \sqrt{\frac{E_{\text{aged}}}{\rho}} \frac{2\rho}{\sigma_{\text{new}} \varepsilon_{\text{new}}} \sqrt{\frac{\rho}{E_{\text{new}}}} \right)^{\frac{1}{3}} \times 100 \\ &= \left(\frac{\sigma_{\text{aged}} \varepsilon_{\text{aged}} \sqrt{\frac{E_{\text{aged}}}{\rho}}}{\sigma_{\text{new}} \varepsilon_{\text{new}} \sqrt{\frac{E_{\text{new}}}{\rho}}} \right)^{\frac{1}{3}} \times 100 \end{aligned} \tag{5}$$

Ballistic materials typically exhibit a linear stress strain curve without any yielding or other nonlinearities, such that

$$E = \frac{\sigma}{\varepsilon}. \tag{6}$$

Substituting Eq. (6) into Eq. (5) gives the expression

$$rV_{50C} = \frac{V_{50C \text{ aged}}}{V_{50C \text{ new}}} \times 100 = \left(\frac{\sigma_{\text{aged}} \varepsilon_{\text{aged}} \sqrt{\frac{\sigma_{\text{aged}} \varepsilon_{\text{new}}}{\sigma_{\text{new}} \varepsilon_{\text{aged}}}}}{\sigma_{\text{new}} \varepsilon_{\text{new}} \sqrt{\frac{\sigma_{\text{new}} \varepsilon_{\text{aged}}}{\sigma_{\text{aged}} \varepsilon_{\text{new}}}}} \right)^{\frac{1}{3}} \times 100 = \left(\frac{\sigma_{\text{aged}}}{\sigma_{\text{new}}} \right)^{\frac{1}{2}} \left(\frac{\varepsilon_{\text{aged}}}{\varepsilon_{\text{new}}} \right)^{\frac{1}{6}} \times 100. \tag{7}$$

From Eq. (7), the rV_{50C} of a material after aging can be determined as a simple function of the aged and unaged ultimate stress and strain.

2.2 Phoenix-Porwal's Tensile-Strength-to- V_{50} Relation

Cunniff derived Eq. (2) and Eq. (3) empirically from extensive data [15]. Taking a theoretical approach, Phoenix and Porwal modeled ballistic impact into a homogeneous, in-plane, isotropic membrane [17, 23]. Their analysis made some assumptions that are inaccurate for ballistic materials; however, their result is surprisingly similar to Cunniff's experimentally determined result. Phoenix and Porwal derived the following relation,

$$V_{50\text{ PP}} = \Omega^{\frac{1}{3}} \frac{2^{\frac{1}{3}} \varepsilon^{\frac{1}{12}} (1 + \theta^2 \Gamma_0)}{K_{\text{max}}^{\frac{3}{4}}}, \tag{8}$$

where Ω and Γ_0 are the same as the variables given in the Cunniff's model, in Eq. (1) and Eq. (3), respectively, θ is an adjustment parameter, typically between 1 and 2, to account for various factors such as plastic projectile nose deformation, fabric wraparound, etc., and K_{max} is given by:

$$K_{\text{max}} = \exp \left\{ -\frac{4\theta^2 \Gamma_0 (\psi_{\text{max}}^2 - 1)}{3(1 + \theta^2 \Gamma_0)} \right\} \psi_{\text{max}}^{\frac{1}{2}} \left[\frac{\sqrt{\frac{\psi_{\text{max}}}{\varepsilon}} (\psi_{\text{max}} - 1)}{\ln \left\{ 1 + \sqrt{\frac{\psi_{\text{max}}}{\varepsilon}} (\psi_{\text{max}} - 1) \right\}} \right]^{\frac{2}{3}}, \tag{9}$$

where ψ_{max} is approximated by

$$\psi_{\text{max}} \approx \sqrt{\frac{1 + \theta^2 \Gamma_0}{2\theta^2 \Gamma_0}}. \tag{10}$$

As above, to predict V_{50} reduction after aging, the projectile-dependent parameters θ , Γ_0 , and ψ_{max} can be held constant, such that

$$V_{50} \propto \Omega^{\frac{1}{3}} \varepsilon^{\frac{1}{12}} \left[\frac{\ln \left\{ 1 + \sqrt{\frac{\psi_{\text{max}}}{\varepsilon}} (\psi_{\text{max}} - 1) \right\}}{\sqrt{\frac{\psi_{\text{max}}}{\varepsilon}} (\psi_{\text{max}} - 1)} \right]^{\frac{1}{2}}. \tag{11}$$

Thus, the retention of V_{50} according to the Phoenix-Porwal model, $rV_{50\text{ PP}}$, is obtained as follows, when using Eq. (8) through Eq. (11):

$$\begin{aligned} rV_{50\text{ PP}} &= \frac{V_{50\text{ PP aged}}}{V_{50\text{ PP new}}} \times 100 = \left(\frac{\Omega_{\text{aged}}}{\Omega_{\text{new}}} \right)^{\frac{1}{3}} \left(\frac{\varepsilon_{\text{aged}}}{\varepsilon_{\text{new}}} \right)^{\frac{1}{12}} \left(\frac{K_{\text{max new}}}{K_{\text{max aged}}} \right)^{\frac{3}{4}} \times 100 \\ &= \left(\frac{\sigma_{\text{aged}}}{\sigma_{\text{new}}} \right)^{\frac{1}{2}} \left(\frac{\varepsilon_{\text{aged}}}{\varepsilon_{\text{new}}} \right)^{\frac{1}{6}} \left(\frac{\varepsilon_{\text{aged}}}{\varepsilon_{\text{new}}} \right)^{\frac{1}{12}} \left[\frac{\sqrt{\frac{\varepsilon_{\text{aged}}}{\varepsilon_{\text{new}}}} \ln \left\{ 1 + \sqrt{\frac{\psi_{\text{max}}}{\varepsilon_{\text{aged}}}} (\psi_{\text{max}} - 1) \right\}}{\ln \left\{ 1 + \sqrt{\frac{\psi_{\text{max}}}{\varepsilon_{\text{new}}}} (\psi_{\text{max}} - 1) \right\}} \right]^{\frac{1}{2}} \times 100, \tag{12} \\ &= \left(\frac{\sigma_{\text{aged}} \varepsilon_{\text{aged}}}{\sigma_{\text{new}} \varepsilon_{\text{new}}} \frac{\ln \left\{ 1 + \sqrt{\frac{\psi_{\text{max}}}{\varepsilon_{\text{aged}}}} (\psi_{\text{max}} - 1) \right\}}{\ln \left\{ 1 + \sqrt{\frac{\psi_{\text{max}}}{\varepsilon_{\text{new}}}} (\psi_{\text{max}} - 1) \right\}} \right)^{\frac{1}{2}} \times 100 \end{aligned}$$

where the rV_{50PP} of a material after aging is a function of the aged and unaged ultimate stress and strain.

2.3 Comparing the Cunniff and Phoenix-Porwal Models

While the Phoenix-Porwal model's V_{50} retention equation, Eq. (12), is more complicated than the Cunniff model's corresponding equation, Eq. (7), the two analyses give remarkably similar results. Taking Eq. (12) and dividing by Eq. (7) gives the factor that differs between these two equations:

$$\frac{rV_{50PP}}{rV_{50C}} = \left(\frac{\varepsilon_{aged}}{\varepsilon_{new}} \right)^{\frac{1}{3}} \left[\frac{\ln \left\{ 1 + \sqrt{\frac{\psi_{max}}{\varepsilon_{aged}}} (\psi_{max} - 1) \right\}}{\ln \left\{ 1 + \sqrt{\frac{\psi_{max}}{\varepsilon_{new}}} (\psi_{max} - 1) \right\}} \right]^{\frac{1}{2}} \quad (13)$$

Furthermore, it can be shown that if $\varepsilon_{aged} < \varepsilon_{new}$, then the V_{50} retention as predicted by the Phoenix-Porwal model in Eq. (12) will be more conservative, i.e., lower, than that predicted by the Cunniff model in Eq. (7).

To enumerate, the full-metal-jacket round nose bullets that were used in this study had nominal masses of 8 g, and their nominal projectile presented area to the target was $A_p = 6.36 \times 10^{-5} \text{ m}^2$. The PPTA and PBO armors had areal densities of 2.625 kg/m² and 2.273 kg/m², respectively, resulting in Γ_0 values of 0.0209 and 0.0181, as shown in Table 1. Table 2 presents values for the ratio in Eq. (13) for the typical ψ_{max} values presented in Table 1.

Table 1. Typical areal density and ψ_{max} values at the indicated θ value for materials used in this study.

	PPTA	PBO
A_d (kg/m ²)	2.63	2.27
A_p (m ²)	6.36E-05	6.36E-05
m_p (g)	8.0	8.0
Γ_0	0.0209	0.0181
$\theta = 1.25$	3.98	4.27
$\theta = 1.5$	3.34	3.58
ψ_{max} $\theta = 1.75$	2.88	3.09
$\theta = 2$	2.55	2.72

Table 2. Typical values of Eq. (13) when $\varepsilon_{new} = 0.03$.

ε_{aged}	$\psi_{max} = 2.5$	$\psi_{max} = 3$	$\psi_{max} = 3.5$	$\psi_{max} = 4$	$\psi_{max} = 4.5$
0.10	1.33	1.35	1.36	1.37	1.37
0.05	1.13	1.14	1.14	1.14	1.15
0.04	1.07	1.08	1.08	1.08	1.08
0.03	1.00	1.00	1.00	1.00	1.00
0.02	0.90	0.90	0.90	0.90	0.90
0.01	0.76	0.75	0.75	0.74	0.74

2.4 Summary

Both Eq. (7) and Eq. (12) relate changes in a material's tensile properties to changes in ballistic properties. These equations were separately derived from theory and empirical testing, yet the ratio in Eq. (13) is around 0.9 to 1.1 (as seen in Table 2), so these models give very similar results. These relations between tensile and ballistic properties allow the ballistic performance of a material to be predicted as the material degrades by performing tensile tests, which require less material and are less costly than ballistic testing.

3. Validation Data: Mechanical Properties and V_{50} Ballistic Performance

To validate the derived theoretical relationships between mechanical properties and ballistic performance, we leveraged data from two different studies. We first examined the effect of degraded material properties on ballistic performance in armor that was subjected to artificial aging protocols within the laboratory. Then, we investigated the relationship between the degradation of material properties in artificially aged laboratory testing to the material properties found in previously fielded armor. All data associated with this publication have been archived at <https://doi.org/10.18434/M32179>.

3.1 Linking Extracted Yarn Tensile Strength to V_{50}

To support the development of a revised NIJ body armor standard [8], armor constructed from two different materials (PBO and PPTA) were subjected to laboratory artificial-aging protocols. Mechanical properties of yarns extracted from these artificially aged vests were obtained, as were ballistic performance measures in the form of V_{50} estimates. In the following sections, we describe the armor, aging, and testing protocols used in the study. We conclude by providing a summary of the analysis and conclusions that relate the degradation in the mechanical properties of extracted yarns to a decrease in ballistic performance.

3.1.1 Armor Description

Two different types of armors were examined herein. One sample armor was constructed of 20 layers of plain woven fabric made from 0.055 g/m (500 denier) PBO yarns, with spacings of 1.02 yarns per mm (26 yarns per inch) in both the horizontal and vertical directions (as extracted from the armor). The layers of fabric were stitched together in two packs of 10 layers each with a 2.54 cm diagonal quilt stitch to form the ballistic package. This ballistic package was then encased in a stitched moisture-permeable fabric cover and inserted into a lightweight polycotton carrier to form an armor panel. This construction was nearly identical to the one that had failed in the field [1, 2, 24].

The other armor was constructed of 25 layers of plain woven 0.055 g/m (500 denier) PPTA, with 0.945 yarns per mm (24 yarns per inch) in both the horizontal and vertical directions. The layers of fabric were stitched together in one package with a 3.18 cm diagonal quilt stitch to form the ballistic package. This ballistic package was then encased in a water-repellent-treated nylon fabric cover and inserted into a medium-weight polycotton carrier to form an armor panel. This armor was selected because it was known to have good long-term field performance. All armors were manufactured specifically for the study. The PBO armor samples were designed to be NIJ Standard 0101.04 Level IIA compliant, and PPTA armor samples were designed to be NIJ Standard 0101.04 Level II compliant [13]. Both armor samples were constructed to be the size required for NIJ Standard 0101.04 2005 Interim Requirements [25] compliance testing.

3.1.2 Artificial Aging

To accelerate the degradation of mechanical properties in the laboratory, the sample armors were simultaneously exposed to elevated temperature, elevated humidity, and mechanical stress through tumbling. The temperature and humidity were held constant throughout the duration of the aging process. Different combinations of temperature, relative humidity (RH), and duration settings were applied to several different test lots (groups) of sample armors. Temperature and relative humidity settings ranged from laboratory ambient conditions (22 °C and 51 % RH) to 70 °C and 90 % RH, and duration settings ranged from 10 d to 13 d. In all cases, the sample armors were tumbled at 0.083 Hz (5 rpm) inside a tumbler that met the specifications of NIJ Standard 0101.06 [8]. The specific aging conditions for each armor lot are provided in Table 3, and further details of the aging conditions can be found in a previous publication [6].

Table 3. Artificial aging conditions.

Lot	Armor Material	Aging Conditions			
		Temp (°C)	Humidity (% RH)	Tumbling (Hz)	Duration (d)
A1	PPTA	--- New armor: no aging ---			
A2	PPTA	22	51	0.083	13
A3	PPTA	65	80	0.083	10
A4	PPTA	70	90	0.083	13
B1	PBO	--- New armor: no aging ---			
B2	PBO	22	51	0.083	13
B3	PBO	65	80	0.083	10
B4	PBO	70	90	0.083	13

3.1.3 Determination of Extracted Yarn Mechanical Properties

To obtain yarn mechanical properties, tensile testing of yarns extracted from the woven fabric inside of the armor was carried out in accordance with ASTM D2256-02 [26], “Standard Test Method for Tensile Properties of Yarn by the Single-Strand Method.” Ten to fifteen yarn specimens from the armors of interest were extracted, and the tensile strength at failure was determined. Testing was performed using a universal test frame equipped with a 91 kg load cell, and pneumatic yarn and cord grips (Instron¹ model 2714-006). The jaw separation was nominally 7.9 cm, and the cross-head speed was approximately 2.3 cm/min. The extracted yarns were nominally 41 cm long and were given 64 twists (1.57 turns/cm or 4 tpi) on a custom-designed yarn-twisting device. This level of twist was maintained on the yarns as they were inserted into the pneumatic yarn and cord grips. Strain measurements were made with a noncontacting video extensometer in conjunction with black foam markers placed approximately 2.5 cm apart in the gauge section of the yarn.

3.1.4 Ballistic Testing

The V_{50} was used as a measure of the armor’s ballistic performance. The V_{50} measurements were executed according to NIJ Standard 0101.04. Because the mechanical properties and the ballistic testing were destructive, no single armor panel could be subjected to both types of measurements. V_{50} measurements were observed from at least one armor panel from each of the test lots with the exception of lot B4, where no V_{50} ballistic data were obtained due to sample constraints.

¹ Certain commercial equipment, instruments, software, or materials are identified in this paper to provide a full description of the procedures used. Such identification does not imply recommendation or endorsement by the National Institute of Standards and Technology, nor does it imply that the materials or equipment identified are necessarily the best available for the purpose.

3.1.5 Results and Discussion

The obtained mechanical property and ballistic performance measurements are shown in Fig. 2. Mechanical properties are also shown in Fig. A1 in Weibull plot format. From the left panel of Fig. 2, we observe that the measured tensile strength values of the new, unaged PBO armor (B1) were substantially larger than those of the new, unaged PPTA armor (A1). This difference in tensile strength diminished rapidly as the armor was aged. The tensile strength of the PBO armor (B1–B4) declined significantly as a result of the artificial aging conditions, whereas the decline in tensile strength was less for the PPTA armor (A1–A4). From the right panel of Fig. 2, we observe that the aging conditions also had a considerable impact on the V_{50} ballistic performance for the PBO armor (B1–B3, no V_{50} data were collected for B4), but little to no impact on the PPTA armor (A1–A4).

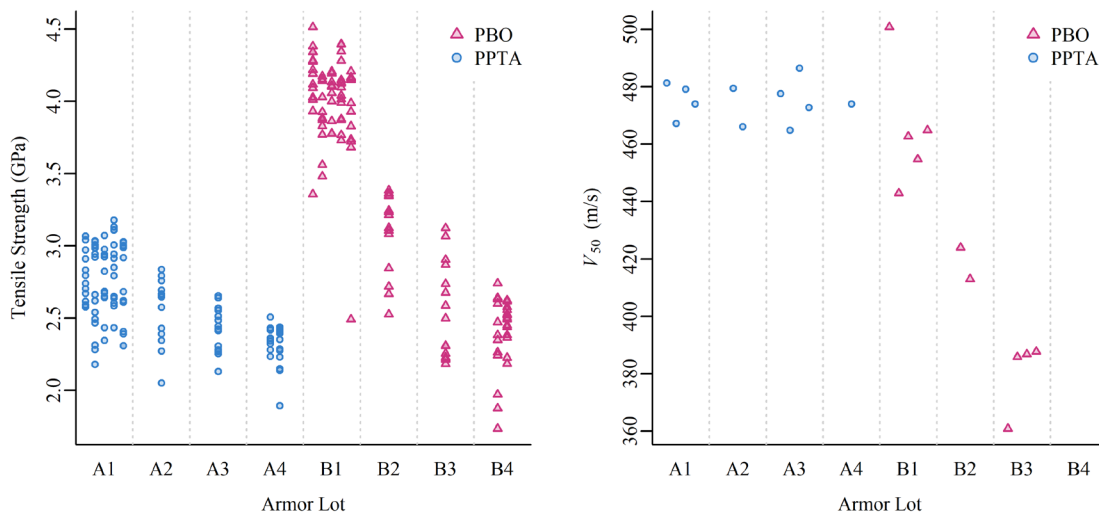


Fig. 2. Left panel: Tensile strength measurements, where multiple fibers were measured from an individual vest to create the vertical stack of data, with results from multiple vests from within a lot illustrated side-by-side. Right panel: Estimated V_{50} values.

Figure 3 displays, for each armor lot, a shaded region that represents the joint interquartile range of the observed tensile strength and ballistic performance measurements. In addition to highlighting the observations noted in the raw data in Fig. 2, Fig. 3 clearly exhibits a positive correlation between tensile strength and ballistic performance for the PBO armor (B1–B3). That is, as the tensile strength of the PBO armor increases, so too does the V_{50} . In contrast, no such trend is observed for the PPTA armor (A1–A4). From these results, we were not able to draw inference on the impact of tensile strength on ballistic performance for PPTA armor because the aging conditions did not impact the PPTA armor in the same manner that they did the PBO armor. This observation could be attributed to a greater variability in strength for lot A1 than the other “A” lots, with a possible greater contribution from these weaker yarns on V_{50} .

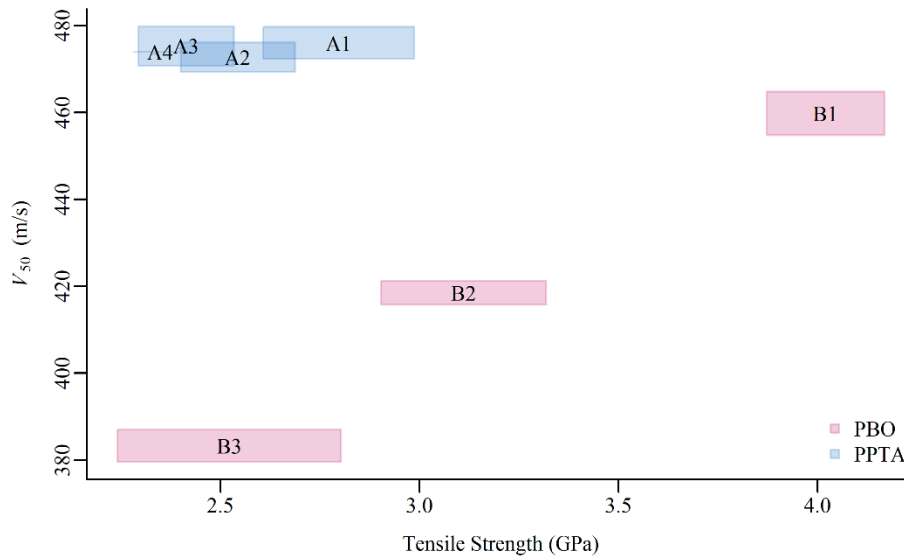


Fig. 3. The joint interquartile range of the observed tensile strength (load at break) and ballistic performance (V_{50}) for each armor lot.

In summary, PBO and PPTA armor were subjected to identical artificial-aging conditions. The tensile strength of the new, unaged PBO armor was about 1.5 times greater than that of the new, unaged PPTA armor. However, the artificial aging had a severe effect on the tensile strength of the PBO armor, while only a slight effect was observed for the PPTA armor. Despite the more favorable tensile strength properties when new, the ballistic performance (V_{50}) of the PBO armor was found to be slightly lower than that of new PPTA armor because the two types of armor were designed to withstand two different NIJ performance levels, as described in Sec. 3.1.1. Similar to the impact on tensile strength, the artificial aging also had a significant influence on the ballistic performance of the PBO armor but not on the ballistic performance of the PPTA armor.

However, it is important to note that armor performance cannot be completely captured by an analysis of material properties. Armor design, including, for example, the number of layers, their interaction with each other and the projectile, and the amount of extra material (or safety margin) built into the vest, is unique for every design, plus design considerations such as stitching and weave type can all influence ballistic results. Therefore, the conclusion that PBO armor was affected by the artificial aging and that PPTA armor was not affected is only valid for a comparison of these two particular armor designs and, in general, is not applicable to all systems containing these materials.

3.2 Linking Properties of Laboratory-Aged Armor to Fielded Armor

While the tensile strength and V_{50} results presented in the previous section indicate a link between mechanical properties of armor materials and ballistic performance, one may consider how these artificially aged laboratory materials are relevant to those observed in fielded armor, especially since the PPTA armor was relatively unchanged by the artificial aging. Accelerated testing through laboratory conditioning of armor is a convenient approach in studying the effect that degraded material properties may have on ballistic performance in fielded armor. Drawing inference from such testing requires that a link be established that illustrates that the laboratory degradation is representative of the degradation that appears in fielded armor. Therefore, we examined results from two studies of material properties (tensile strength) of fielded armor and compared them to the artificially aged armor results presented in the previous section.

3.2.1 Armor Description

Tensile strength measurements from fielded PPTA armor were obtained through research efforts performed in conjunction with the Canadian government [9, 10]. The field-worn Canadian police armors were all manufactured by the same parent company and were composed entirely of PPTA yarns. The manufacturing date of the panels spanned a 10 year period from October 1992 to October 2002.

The material properties of fielded PBO armor were examined as part of Phase II of the U.S. Department of Justice's Body Armor Safety Initiative [1–3, 5, 24]. The 75 fielded PBO-containing body armor pieces collected for this effort varied in age (17 to 71 months), material composition (15 % PBO to 100 % PBO), NIJ threat certification (IIA–IIIA), manufacturer, general condition, and geographic area of use.

3.2.2 Determination of Extracted Yarn Mechanical Properties

Forty-one armor panels of interest from the Canadian PPTA work were selected for mechanical properties testing. These panels were selected because they were all from the same model of armor. Approximately 14 yarns were extracted from each PPTA armor panel and subjected to material properties testing using the procedure described above in Sec. 3.1.3. The tensile strength results for the 577 total PPTA yarn specimens are provided in the following section.

For the PBO armor, a total of 52 yarns were extracted from 10 fielded PBO-containing armor panels. In the cases where the armor contained materials other than PBO, only yarns containing PBO were extracted and subjected to mechanical properties testing. As with the PPTA mechanical properties testing, the PBO yarn tensile strength was measured using the procedure described above in Sec. 3.1.3. The tensile strength results for the 52 total PBO yarn specimens are provided in the following section.

3.2.3 Analysis and Discussion

Figure 4 provides the distribution of the tensile strength measurements of the fibers extracted from the field-worn armor (histograms) compared to the tensile strength measurements from the laboratory artificially aged armor (box plots). The tensile strength data for both the fielded PPTA and the fielded PBO armor approximately follow a normal distribution. The tensile strength measurements for the fielded PPTA armor were tightly gathered around the mean of 2.84 GPa, with a standard deviation of 0.24 GPa, for a coefficient of variation (CV) of 8.5 %. The observed minimum and maximum fielded PPTA tensile strength measurements were 2.15 GPa and 3.43 GPa, respectively. Conversely, the tensile strength measurements for the fielded PBO armor were much more spread around the mean of 2.64 GPa, with a standard deviation of 0.61 GPa, for a CV of 23.1 %. The observed minimum and maximum fielded PBO tensile strength measurements were 1.41 GPa and 3.93 GPa, respectively. The observation of a larger spread of tensile strengths in PBO than in PPTA armor was also noted in the laboratory artificially aged armor. This implies that aging and environmental conditions, both field and laboratory induced, have a smaller impact on yarns extracted from PPTA armor as compared to yarns extracted from PBO armor.

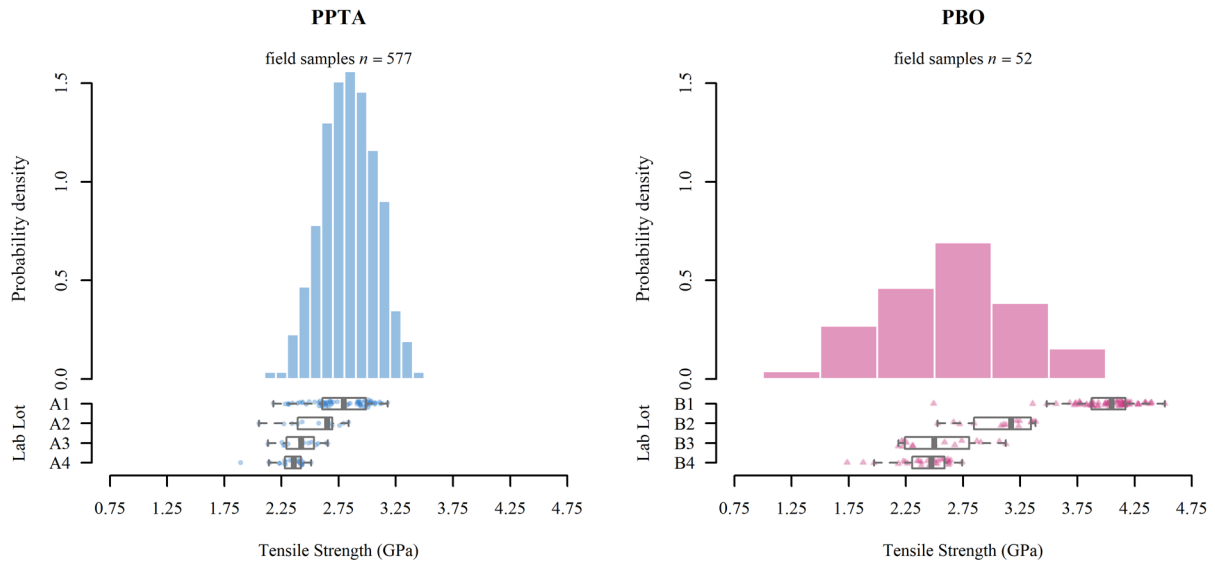


Fig. 4. Tensile strength testing results for PPTA (left) and PBO (right) armor. The histograms illustrate the probability density functions of the tensile strength for the field-worn armor, and the box plots with individual data points provide the tensile strength of the laboratory artificially aged armor.

In comparing the tensile strength measurements of the new, unaged PPTA armor from the laboratory aging study (Lab Lot A1) to the distribution of fielded PPTA tensile strength measurements, we observe from the left panel of Fig. 4 that the unaged laboratory armor was generally reflective of the fielded armor. While the laboratory artificial aging slightly reduced the tensile strength of the PPTA armor (Lab Lots A2–A4), the values remained consistent with the lower half of the distribution of fielded PPTA tensile strength measurements.

Conversely, when comparing the tensile strength measurements of the PBO armor from the laboratory aging study to the distribution of fielded PBO armor tensile strength measurements (right panel of Fig. 4), the tensile strength of the new, unaged PBO armor (Lab Lot B1) is reflective of only the strongest of the fielded PBO tensile strength measurements. Because the fielded PBO armor was a random sample from in-use armor, this suggests that most fielded PBO armor examined herein had experienced significant degradation in tensile strength. We observed that the laboratory artificial aging significantly reduced the tensile strength of the PBO armor (Lots B2–B4), but still, the weakest of the aged lots (B3 and B4) were reflective of the middle part of the yarn strength distribution for yarns extracted from the fielded PBO armor samples. Recall that the ballistic performance of these lots, particularly B2 and B3, was drastically lower than for the new armor lot (B1). There remains a significant proportion of the fielded PBO tensile strength distribution that exhibited lower tensile strength than even the weakest laboratory-aged lots.

In summary, while the PPTA armor only saw minor reductions in tensile strength and ballistic performance when exposed to the laboratory artificial aging conditions described in Sec. 3.1.2, the observed diminished tensile strength values were determined to be reflective of the more degraded field-worn PPTA armor. Any further reduction in tensile strength through additional artificial aging conditions would have pushed the degradation of the armor beyond what was seen in the field. This observed lack of decline in tensile strength and ballistic performance may be attributed to the robustness of the PPTA material to the aging and environmental conditions to which it was exposed. Conversely, despite the large degradation effect of laboratory artificial aging on PBO yarn strength, more aging would be required to be reflective of the lower portion of the tensile strength distribution of the fielded PBO armor. Though the observed tensile strength reduction from the artificially aged PBO armor does not conflict with that observed in the fielded armor, more aggressive laboratory aging would be required to fully reflect the tensile strength loss in extracted yarn samples from the most degraded field-worn PBO armor.

In this section, we have presented studies that demonstrate the effect of degraded material properties on ballistic performance in armor, and we have linked the degradation observed in the laboratory artificially aged armor to that found in fielded armor. Next, we used these data to demonstrate how the theoretical degradation relationships developed in Sec. 2 may be applied to predict ballistic performance from more easily measured mechanical properties.

4. Validation Results: Predicting Armor Performance Using Dimensional Analysis

As previously discussed, dimensional analysis relating the properties of fiber strain-wave speed and specific toughness [14–19] can be used to predict a theoretical V_{50} . This concept could be a powerful tool in predicting the effect of a change in fiber properties (such as changes in tensile strength, elongation at break, or modulus due to aging) on the ballistic performance of an armor system. This theoretical V_{50} could then be used to determine when a change in the material properties measured from an armor sample might translate into a loss in performance in the case of field and laboratory aging studies, or an increase in performance in the case of new or improved fibers.

Sometimes, only very limited data or samples are available from a fielded or laboratory-aged armor, and it is not possible to conduct extensive V_{50} testing. In order to develop a V_{50} with reasonable confidence, multiple panels should be tested, but large sample sizes might not be available, particularly ones that have been subjected to identical environments and service in the field. In these cases, where multiple yarns can be extracted from a single armor sample, a theoretically determined V_{50} could potentially be used to determine some point, perhaps a conservative one, at which measured degradation in mechanical properties might translate into a critical reduction in ballistic performance. However, the relationship between the theoretically predicted performance and actual measured performance must be understood before the value of this approach can be realized.

Regarding such theoretical estimations of V_{50} from yarn strength data, it is critical to emphasize that the purpose is not to determine absolute values of V_{50} , for any particular armor, but instead, the purpose is to determine relative V_{50} behavior in ratio form, whereby the influence of degradation in mechanical material properties of the key armor materials on its ballistic performance is assessed, all other things being equal.

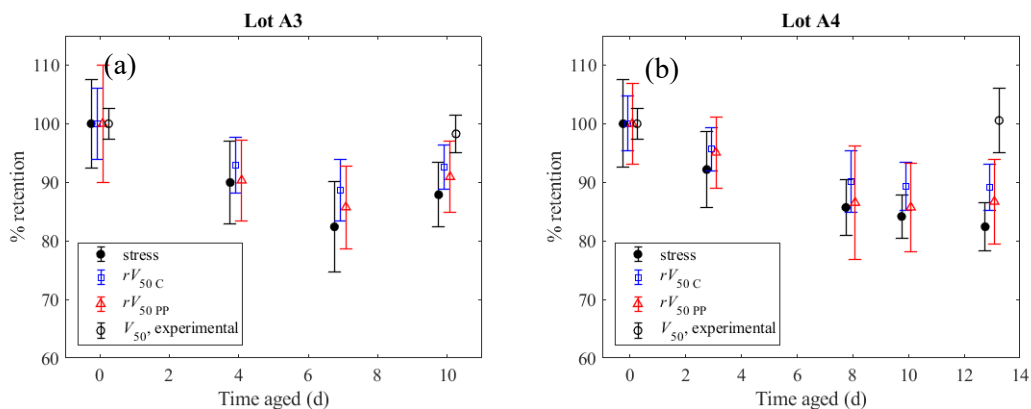


Fig. 5. Tensile strength retention and V_{50} retention, relative to the initial, unaged values, as computed using both the Cunniff (C) model and the Phoenix-Porwal (PP) model. Predicted and measured V_{50} values are shown for PPTA armor (a) Lot A3 and (b) Lot A4 (see Table 3 for environmental conditioning). Error bars represent the 95 % confidence interval for the scale parameter from a logistic fit of the experimental V_{50} data, and standard deviation of an average of at least 10 measurements, scaled by the initial mean, for the other lines. Values in (a) and (b) are tabulated in Table A1 and Table A2, respectively.

To examine this relationship, the predicted V_{50} based on material properties measured from yarn specimens from the aged armor was compared with actual measured ballistic limit results from armor exposed in the same manner, using the V_{50} of the aged armor divided by the original V_{50} , the ratio called V_{50} retention. Figures 5 and 6 show, in ratio form, yarn tensile strength retention, predicted V_{50} retention, using both the Cunniff and Phoenix-Porwal methods from Eq. (7) and Eq. (12), respectively, and last, actual V_{50} retention for aged samples. For the Phoenix-Porwal model, ψ_{\max} was fixed at 2.87. Tables A1 through A4, in the Appendix, give ratio values for tensile strength retention, failure strain retention, and predicted V_{50} retention using both the Cunniff model and the Phoenix-Porwal model. Large error bars on the Phoenix-Porwal's V_{50} retention typically are due to uncertainty in strain values, as can be seen in the table associated with the figure. The influence of the strain on Phoenix-Porwal's V_{50} retention is also why it does not always follow the same trend as the tensile strength and Cunniff's V_{50} retention. Cunniff's V_{50} retention is influenced much less by the failure strain and thus typically matches the trends of the failure stress.

Yarns extracted from the PPTA armor from Lot A4 exhibited a decline in tensile strength of approximately 18 %, and the armor from Lot A3 exhibited a decline of approximately 11 %. In both cases, the actual measured V_{50} of the PPTA armor was relatively unchanged by the conditioning protocols. The predicted V_{50} showed a theoretical decline of approximately 11 % and 13 % for the Cunniff model and the Phoenix-Porwal model, respectively, for Lot A4, and a theoretical decline of approximately 7 % and 9 % for the Cunniff model and the Phoenix-Porwal model, respectively, for Lot A3. It is interesting to note that the predicted V_{50} consistently provided a conservative estimate of the V_{50} of the degraded PPTA system, and that the predicted ratio appears to be more sensitive to changes in tensile strength for this system than the actual measured V_{50} . This may be attributed to the differences in material behavior at the slow, quasi-static rates where the tensile testing is performed, as compared to the extremely fast time scale of the ballistic tests. In addition, changes such as material susceptibility to mechanical damage and armor design are not considered in these models. Furthermore, the Phoenix-Porwal model is more conservative than the Cunniff model, which is consistent with the factor in Eq. (13) being less than unity in the case where the failure strain after aging is less than the failure strain before aging. These results demonstrate that the PPTA system examined here is robust and can withstand some yarn material degradation before changes in experimentally determined V_{50} are observed.

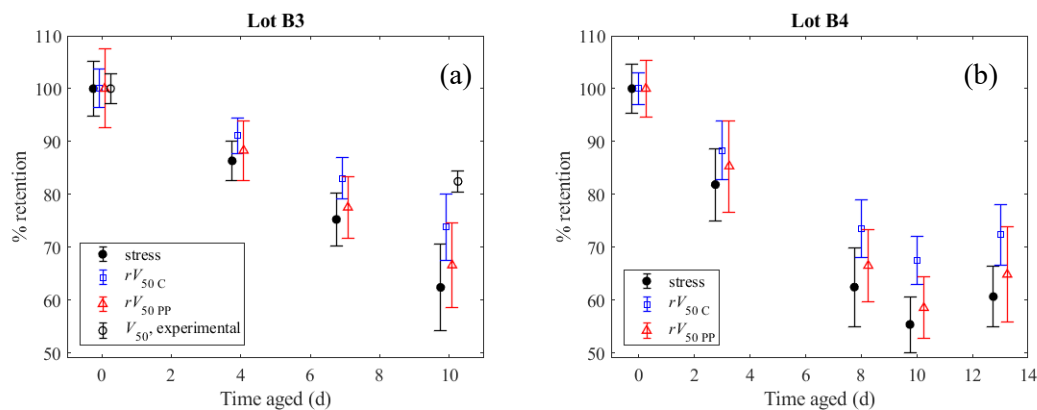


Fig. 6. Tensile strength retention, predicted V_{50} retention, and measured V_{50} reduction relative to the initial, unaged values for PBO armor (a) Lot B3 and (b) Lot B4 (see Table 3 for environmental conditioning). Error bars represent the 95 % confidence interval for the scale parameter from a logistic fit of the experimental V_{50} data, and standard deviation of an average of at least 10 measurements, scaled by the initial mean, for the other lines. Values in (a) and (b) are tabulated in Table A3 and Table A4, respectively.

This analysis was also applied to similar data sets for the PBO armor. Figure 6 shows tensile strength retention, predicted V_{50} retention, and measured V_{50} retention for aged PBO samples. Yarns extracted from the PBO armor from Lot B4 exhibited an approximate reduction in tensile strength of 40 % after exposure,

and the armor from Lot B3 exhibited a reduction in tensile strength of approximately 38 % after exposure. In both cases, the actual measured V_{50} of the PBO armor was reduced by 15 % to 18 % by the aging. The predicted V_{50} showed a theoretical decline of 28 % and 35 % for the Cunniff model and the Phoenix-Porwal models, respectively. For Lot B4, the corresponding V_{50} declines were 26 % and 33 % for the Cunniff and the Phoenix-Porwal models, respectively, for Lot B3.

In summary, the theoretical predictions for V_{50} follow the same trends as the tensile properties with aging and provide conservative estimates for the measured V_{50} for both the PPTA and PBO armors. The two different theoretical methods predict similar results, differing by less than 5 % in predicted V_{50} reduction.

5. Conclusions and Future Work

In conclusion, there appears to be a correlation between changes in mechanical properties and changes in ballistic performance for PBO armor exposed to different aging conditions. This relationship is not observed for PPTA armor when aged under the same conditions. Theoretical V_{50} values were calculated for new and aged PPTA and PBO armor systems and compared to the actual change in ballistic performance. Both Cunniff's and Phoenix-and-Porwal's equations for theoretical V_{50} appeared to provide a conservative estimate of the change in ballistic performance for both PPTA and PBO armor.

This work raises the possibility of an opportunity to include an "armor witness coupon sample" made up of extra material from the armor and inserted into the ballistic panel, where it could be easily sampled. Material properties from this coupon sample when new could be cataloged in a database for future reference. This coupon sample could then be removed from the armor panel and its material properties analyzed later in the vest's service lifetime. Then, V_{50} could be computed and compared to the original material parameters. This approach could serve as a useful tool for fielded armor performance surveillance programs relying upon testing of armor coupon samples. While this study has provided some information, more analyses of field-aged and laboratory-aged armor systems are critical to fully understand and predict armor service life, especially as commonly used fibers are improved and new fibers and technologies are introduced into the marketplace.

6. Appendix A

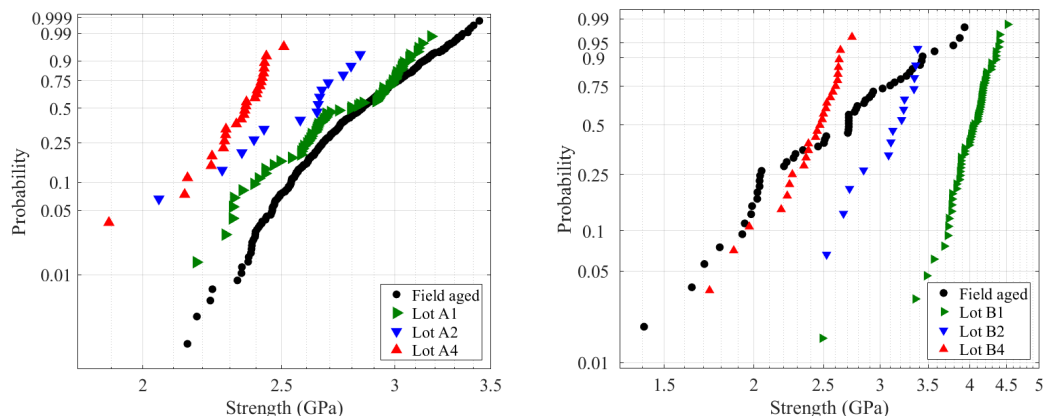


Fig. A1. Tensile strength plotted on a Weibull probability plot, for PPTA (left) and PBO (right), comparing field-aged samples with laboratory-aged samples.

In the tables below, the mean is denoted by μ ; the standard deviation is denoted by σ ; the normalized mean is denoted by μ_n , where $\mu_n = \mu_t / \mu_0$, and where μ_0 is the mean at day 0, and the coefficient of variation is denoted by CV , where $CV = \mu / \sigma$.

Table A1. Tensile stress retention, V_{50} retention relative to the initial, unaged values, as computed using both the Cunniff model and the Phoenix-Porwal (P & P) model, and measured V_{50} for PPTA armor from Lot A3. Values with a subscript ‘n’ are normalized by the initial mean on day 0. Values are the average of at least 13 tensile tests.

Day	Stress				Strain				Cunniff		P & P	
	μ (GPa)	σ (GPa)	μ_n (%)	CV	μ (%)	σ (%)	μ_n (%)	CV	μ_n (%)	CV	μ_n (%)	CV
0	2.76	0.209	1.000	13.2	2.68	0.996	1.000	2.69	1.000	16.5	1.000	9.95
4	2.48	0.194	0.900	12.8	2.59	0.318	0.966	8.15	0.930	19.6	0.903	13.2
7	2.27	0.212	0.824	10.7	2.54	0.281	0.947	9.04	0.887	17.1	0.858	12.1
10	2.42	0.152	0.879	15.9	2.71	0.342	1.009	7.92	0.926	24.4	0.909	15.1

Table A2. Tensile stress retention, V_{50} retention using both the Cunniff model and the Phoenix-Porwal (P & P) model, and measured V_{50} for PPTA armor from Lot A4. Values with a subscript ‘n’ are normalized by the initial mean on day 0. Values are an average from two different samples, each consisting of at least 13 tensile tests.

Day	Stress				Strain				Cunniff		P & P	
	μ (GPa)	σ (GPa)	μ_n (%)	CV	μ (%)	σ (%)	μ_n (%)	CV	μ_n (%)	CV	μ_n (%)	CV
0	2.84	0.212	1.000	13.4	2.99	0.340	1.000	8.79	1.000	21.4	1.000	14.5
3	2.62	0.183	0.922	14.3	2.94	0.454	0.982	6.47	0.956	26.3	0.951	15.6
8	2.43	0.133	0.857	18.3	2.56	0.570	0.857	4.50	0.901	17.2	0.865	8.96
10	2.39	0.105	0.842	22.7	2.55	0.425	0.853	6.00	0.893	21.6	0.857	11.3
13	2.34	0.117	0.824	19.9	2.69	0.459	0.899	5.86	0.891	22.5	0.867	11.9

Table A3. Tensile stress retention, V_{50} retention using both the Cunniff model and the Phoenix-Porwal (P & P) model, and measured V_{50} reduction relative to the initial, unaged values for PBO from Lot B3. Values with a subscript ‘n’ are normalized by the initial mean on day 0. Values are the average of at least 13 tensile tests.

Day	Stress				Strain				Cunniff		P & P	
	μ (GPa)	σ (GPa)	μ_n (%)	CV	μ (%)	σ (%)	μ_n (%)	CV	μ_n (%)	CV	μ_n (%)	CV
0	4.08	0.213	1.000	19.1	2.59	0.404	1.000	6.42	1.000	27.4	1.000	13.4
4	3.52	0.153	0.863	23.0	2.28	0.260	0.880	8.76	0.911	27.1	0.883	15.6
7	3.07	0.204	0.752	15.1	1.98	0.258	0.763	7.68	0.830	21.2	0.775	13.1
10	2.55	0.332	0.624	7.7	1.73	0.275	0.665	6.270	0.738	11.8	0.666	8.32

Table A4. Tensile stress retention, V_{50} retention using both the Cunniff model and the Phoenix-Porwal (P & P) model, and measured V_{50} reduction relative to the initial, unaged values for PBO from Lot B4. Values with a subscript 'n' are normalized by the initial mean on day 0. Values are an average from two different samples, each consisting of at least 13 tensile tests.

Day	Stress				Strain				Cunniff		P & P	
	μ (GPa)	σ (GPa)	μ_n (%)	CV	μ (%)	σ (%)	μ_n (%)	CV	μ_n (%)	CV	μ_n (%)	CV
0	3.96	0.186	1.000	21.3	2.79	0.333	1.000	8.36	1.000	34.0	1.000	18.6
3	3.24	0.270	0.818	12.0	2.43	0.397	0.871	6.11	0.883	15.8	0.853	9.86
8	2.47	0.294	0.624	8.39	1.86	0.286	0.669	6.51	0.736	13.5	0.665	9.71
10	2.19	0.209	0.553	10.5	1.59	0.245	0.569	6.48	0.675	15.1	0.585	10.0
13	2.40	0.229	0.606	10.5	1.82	0.445	0.653	4.09	0.723	12.6	0.648	7.23

Acknowledgments

Financial support for this research effort was provided by the National Institute of Justice under Interagency Agreement Number 2003-IJ-R-029. Their support is gratefully acknowledged. Financial support for A.E.W. was provided under National Institute of Standards and Technology cooperative agreements NIST 70NANB17H337 and 70NANB18H222. We would also like to thank our dear friend and colleague Kirk Rice for his guidance, support, and assistance in this work.

7. References

- [1] National Institute of Justice (2004) Status Report to the Attorney General of Body Armor Safety Initiative Testing and Activities (National Institute of Justice, Washington, DC). NIJ Special Report. Available at <https://www.ojp.usdoj.gov/nij>
- [2] National Institute of Justice (2004) Supplement I: Status Report to the Attorney General of Body Armor Safety Initiative Testing and Activities (National Institute of Corrections, Washington, DC). NIJ Special Report. Available at <https://www.ojp.usdoj.gov/nij>
- [3] National Institute of Justice (2005) Third Status Report to the Attorney General on Body Armor Safety Initiative Testing and Activities (National Institute of Corrections, Washington, DC). NIJ Special Report. Available at https://ojp.gov/bvpbasi/docs/SupplementII_08_12_05.pdf
- [4] Frank D (1986) Ballistic Tests of Used Soft Body Armor (National Bureau of Standards, Gaithersburg, MD). NBSIR 86-3444. <https://doi.org/10.6028/NBS.IR.86-3444>
- [5] Chin J, Byrd E, Clerici C, Oudina M, Sung L, Forster AL, Rice K, Stutzman P (2007) Chemical and Physical Characterization of Poly(*p*-phenylene-2,6-benzobisoxazole) Fibers Used in Body Armor Used in Body Armor: Temperature and Humidity Aging (National Institute of Standards and Technology, Gaithersburg, MD). NISTIR 7373. <https://doi.org/10.6028/NIST.IR.7373>
- [6] Forster AL, Rice KD, Riley MA, Messin GHR, Petit S, Clerici C, Vigoroux MC, Pintus P, Holmes G, Chin J (2009) Development of Soft Armor Conditioning Protocols for NIJ Standard 0101.06: Analytical Results (National Institute of Standards and Technology, Gaithersburg, MD). NISTIR 7627. <https://doi.org/10.6028/NIST.IR.7627>
- [7] Forster AL, Pintus P, Messin G, Riley MA, Petit S, Rossiter W, Chin J, Rice KD (2011) Hydrolytic stability of polybenzobisoxazole and polyterephthalamide body armor. *Polymer Degradation and Stability* 96(2):247–254. <https://doi.org/10.1016/j.polydegradstab.2010.10.004>
- [8] National Institute of Justice (2008) *NIJ Standard 0101.06 Ballistic Resistance of Body Armor* (U.S. Department of Justice, Office of Justice Programs, Washington, DC).
- [9] Withnall C, Garland L, Bourget D (2010) Aged body armour testing in development of a replacement protocol. *Proceedings of the 10th Personal Armour Systems Symposium* (Quebec City, Quebec, Canada).
- [10] Bourget D, Withnall C, Palmer S, Rice KD, Swann S (2012) Aged body armour testing: Further results. *Proceedings of the 11th Personal Armour Systems Symposium* (Nuremberg, Germany).
- [11] ASTM (2018) *ASTM E3110-18--Standard Test Method for Collection of Ballistic Limit Data for Ballistic-Resistant Torso Body Armor and Shoot Packs* (ASTM International, West Conshohocken, PA). Available at <https://www.astm.org/DATABASE.CART/HISTORICAL/E3110-18.htm>
- [12] Mauchant D, Rice K, Riley M, Leber D, Samarov D, Forster A (2011) Analysis of Three Different Regression Models to Estimate the Ballistic Performance of New and Environmentally Conditioned Body Armor (National Institute of Standards and Technology, Gaithersburg, MD). NISTIR 7760. <https://doi.org/10.6028/NIST.IR.7760>

- [13] NIJ (2000) *NIJ Standard 0101.04 Ballistic Resistance of Personal Body Armor* (National Institute of Justice, Washington, DC). Available at <https://www.ncjrs.gov/pdffiles1/nij/183651.pdf>
- [14] Hearle JWS (2001) *High Performance Fibers* (Woodhead Publishing, Cambridge, UK).
- [15] Cunniff PM (1999) Dimensionless parameters for optimization of textile-based armor systems. *18th International Symposium on Ballistics* (San Antonio, TX), pp 1302–1310.
- [16] Phoenix S, Porwal P (2003) A new membrane model for the ballistic impact response and V_{50} performance fo multi-ply fibrous systems. *International Journal of Solids and Structures* 40(24):6723–6765. [https://doi.org/10.1016/S0020-7683\(03\)00329-9](https://doi.org/10.1016/S0020-7683(03)00329-9)
- [17] Porwal P, Phoenix S (2005) Modeling system effects in ballistic impact into multi-layered fibrous materials for soft body armor. *International Journal of Fracture* 135:217–249. <https://doi.org/10.1007/s10704-005-3993-9>
- [18] Porwal P, Phoenix SL (2008) Effects of layer stacking order on the V_{50} velocity of a two-layered hybrid armor system. *Journal of Mechanics of Materials and Structures* 3:627. <https://doi.org/10.2140/JOMMS.2008.3.627>
- [19] McDonough WG, Holmes GA, Forster AL, Rice KD (2010) A graphical approach for assessing high-strength fiber performance. *SAMPE 2010 Annual Technical Conference* (Boston, MA), p 9.
- [20] McDonough WG, Forster AL, Kim JH, Heckert NA, Dunkers JP, Wight SA, Holmes GA (2015) The testing program at NIST on fibers used in soft body armor applications. *Annual Technical Conference (ANTEC), Conference Proceedings* (Orlando, FL).
- [21] Engelbrecht-Wiggans A, Burni F, Krishnamurthy A, Forster AL (2020) Tensile testing of aged flexible unidirectional composite laminates for body armor. *Journal of Materials Science* 55(3):1035–1048. <https://doi.org/10.1007/s10853-019-04063-w>
- [22] Obaid AA, Deitzel JM, Gillespie JW, Zheng JQ (2011) The effects of environmental conditioning on tensile properties of high performance aramid fibers at near-ambient temperatures. *Journal of Composite Materials* 45(11):1217–1231. <https://doi.org/10.1177/0021998310381436>
- [23] Leigh Phoenix S, Porwal PK (2003) A new membrane model for the ballistic impact response and V_{50} performance of multi-ply fibrous systems. *International Journal of Solids and Structures* 40(24):6723–6765. [https://doi.org/10.1016/S0020-7683\(03\)00329-9](https://doi.org/10.1016/S0020-7683(03)00329-9)
- [24] Chin J, Byrd E, Forster AL, Gu X, Nguyen T, Scierka S, Sung L, Stutzman P, Sieber J, Rice K (2006) NISTIR 7237: Chemical and Physical Characterization of Poly(*p*-phenylene-2,6-benzobisoxazole) Fibers Used in Body Armor (National Institute of Standards and Technology, Gaithersburg, MD). NISTIR 7237. <https://doi.org/10.6028/NIST.IR.7237>
- [25] National Institute of Justice (2005) *NIJ Standard 0101.04 2005 Interim Requirements: Ballistic Resistance of Personal Body Armor* (National Institute of Justice, Washington, DC).
- [26] ASTM (2002) *ASTM D2256-02 Standard Test Method for Tensile Properties of Yarn by the Single-Strand Method* (ASTM International, West Conshohocken, PA). Available at <https://www.astm.org/DATABASE.CART/HISTORICAL/D2256-02.htm>

About the authors: Amanda L. Forster is a materials research engineer in the Materials Measurement Science Division at NIST. Dennis D. Leber is a mathematical statistician in the Statistical Engineering Division at NIST. Amy Engelbrecht-Wiggans is a guest researcher in the Materials Measurement Science Division at NIST. Virginie Landais, Allen Chang, Emilien Guigues, and Guillaume Messin are former guest researchers in the Materials Measurement Science Division at NIST. Michael A. Riley is a research engineer in the Materials Measurement Science Division at NIST. The National Institute of Standards and Technology is an agency of the U.S. Department of Commerce.